



Modular control of human walking: Adaptations to altered mechanical demands

Craig P. McGowan^{a,*}, Richard R. Neptune^a, David J. Clark^b, Steven A. Kautz^{b,c,d}

^a Department of Mechanical Engineering, The University of Texas at Austin, Austin, TX 78712, USA

^b Brain Rehabilitation Research Center Malcom Randall VA Medical Center, Gainesville, FL, USA

^c Department of Physical Therapy, University of Florida, Gainesville, FL, USA

^d Brooks Center for Rehabilitation Studies, University of Florida, Gainesville, FL, USA

ARTICLE INFO

Article history:

Accepted 5 October 2009

Keywords:

Forward dynamic simulation
Weight support
Load carrying
Muscles synergies
Biomechanical function

ABSTRACT

Studies have suggested that the nervous system may adopt a control scheme in which synergistic muscle groups are controlled by common excitation patterns, or modules, to simplify the coordination of movement tasks such as walking. A recent computer modeling and simulation study of human walking using experimentally derived modules as the control inputs provided evidence that individual modules are associated with specific biomechanical subtasks, such as generating body support and forward propulsion. The present study tests whether the modules identified during normal walking could produce simulations of walking when the mechanical demands were substantially altered. Walking simulations were generated that emulated human subjects who had their body weight and/or body mass increased and decreased by 25%. By scaling the magnitude of five module patterns, the simulations could emulate the subjects' response to each condition by simply scaling the mechanical output from modules associated with specific biomechanical subtasks. Specifically, the modules associated with providing body support increased (decreased) their contribution to the vertical ground reaction force when body weight was increased (decreased) and the module associated with providing forward propulsion increased its contribution to the positive anterior–posterior ground reaction force and positive trunk power when the body mass was increased. The modules that contribute to controlling leg swing were unaffected by the perturbations. These results support the idea that the nervous system may use a modular control strategy and that flexible modulation of module recruitment intensity may be sufficient to meet large changes in mechanical demand.

© 2009 Elsevier Ltd. All rights reserved.

1. Introduction

Walking is an exceedingly complex control problem which requires the coordination of a musculoskeletal system with highly non-linear properties. The body has more muscles than kinematic degrees of freedom and some muscles span multiple joints. Further, as a result of dynamic coupling, it is possible for muscles to accelerate joints and segments that they do not span (e.g., Zajac et al., 2003). However, a number of recent studies using factor analyses of surface electromyography (EMG) suggest that the nervous system may adopt a relatively simple control strategy (e.g., Cappellini et al., 2006; Clark et al., 2009; Ivanenko et al., 2005). Indeed, both the disparate patterns of activation observed across muscles and the variability of activation across steps can be accounted for by combining and scaling a small set of basic activation patterns. These patterns, or modules, have been identified using a number of factorization techniques and have

shown consistency over a wide range of walking speeds (e.g., Cappellini et al., 2006; Clark et al., 2009; Ivanenko et al., 2004), during tasks such as stepping and kicking (Ivanenko et al., 2005) and when walking with body weight support (Ivanenko et al., 2004).

A number of studies have provided evidence that individual modules may be associated with specific biomechanical output (e.g., Davis and Vaughan, 1993; Ting and Macpherson, 2005), although identifying the biomechanical function associated with each module is difficult to test or measure directly. Recently, we used experimentally derived modules in a forward dynamics simulation of walking to identify the biomechanical functions associated with each module (Neptune et al., 2009). Four primary modules were identified from EMG activity from healthy adults (Clark et al., 2009) and the activation pattern for each module was used as the control input for the muscles belonging to that module. Analyzing muscle contributions to the ground reaction forces (GRF) and body segment mechanical energetics, each module was found to be associated with specific biomechanical functions. Module 1 (hip and knee extensors) provided body support in early stance while module 2 (ankle plantar flexors) contributed to body support and forward propulsion in late

* Corresponding author. Tel.: +1 512 471 0848.

E-mail address: cpmcgowan@mail.utexas.edu (C.P. McGowan).

stance. Module 3 (tibialis anterior and rectus femoris) acted to decelerate the leg during early and late swing and generated power to the trunk throughout the swing phase. Module 4 (hamstrings) also acted to decelerate the leg in late swing and generated energy to the leg in early stance. The analysis also revealed a fifth module (iliopsoas) to be present and active in accelerating the leg forward during swing. However, because these modules were defined during steady-state walking conditions, it is not clear whether they are sufficiently robust to perform different walking tasks when the mechanical demands are substantially altered.

In the present study, we generated simulations emulating human subjects who had their body weight and/or body mass increased and decreased by 25%. Perturbations of this magnitude have been shown to produce statistically significant changes in a number of variables including ground reaction forces, joint moments, EMG activity and metabolic cost (e.g., Grabowski et al., 2005; McGowan et al., 2008), and therefore impose a quantifiable change in demand on the musculoskeletal system. Adding trunk loads increased both body weight and body mass, thus increasing the demand for body support and forward propulsion. Weight support decreased the demand for body support but did not alter the demand for forward propulsion because body mass was unchanged. The equal combination of added trunk loads and weight support increased the mass that had to be propelled forward without increasing the weight that had to be supported. We expected modules that have been shown to be associated with specific subtasks would increase or decrease their activation in response to changes in demand for those tasks. Specifically, we hypothesized that the module controlling body support would increase or decrease activation with changes in body weight, while the module controlling forward propulsion would be sensitive to manipulations of both body weight and body mass. Finally, because the mass of the limbs was not altered, we hypothesized that the module controlling leg swing would be similar to the nominal control simulation. Using these simulation analyses, we will be able to test the hypothesis that a reduced set of control inputs can robustly reproduce walking mechanics under different biomechanical conditions.

2. Methods

2.1. Experimental data

The human subject experimental apparatus, protocol, and data processing for body weight and body mass manipulations have been previously described in detail (McGowan et al., 2008). The control condition and 25% manipulations from McGowan et al. (2008) were used in the current study. Data were collected from ten healthy subjects (5 male/5 female; height = 1.74 ± 0.09 m; mass = 67.1 ± 8.5 kg; age = 27.7 ± 7.7 yrs) walking at 1.3 ms^{-1} on a dual belt force measuring treadmill. All subjects provided informed consent prior to data collection. Subjects walked normally (control) and with added trunk loads (increased weight and mass), weight support (decreased weight only), and an equal combination of added trunk load and weight support (increased mass only) for a total of four conditions. Weight support was provided by a custom-built apparatus that supplied a nearly constant upward force via a long, low-stiffness spring (McGowan et al., 2008). Sagittal plane kinematics and ground reaction forces were collected at 200 and 2000 Hz, respectively and standard inverse dynamics techniques were used to calculate joint moments and powers. Data from ten consecutive steps were averaged within subjects and then across subjects to obtain a group average for each condition.

2.2. Musculoskeletal model

To generate simulations of the experimental conditions above, a previously described musculoskeletal model and simulation framework were used (e.g., Neptune et al., 2004, 2009). Briefly, the model was developed using SIMM (MusculoGraphics, Inc.) and was composed of rigid segments consisting of a trunk and two legs, with each leg having a thigh, shank, patella, rear-foot, mid-foot and

toes. The model had 13 degrees of freedom including flexion/extension at the hip, knee, ankle, mid-foot and toes of each leg, and horizontal and vertical translation and pitch rotation at the trunk. Foot-ground contact was modeled using 30 viscoelastic elements with Coulomb friction (Neptune et al., 2000) distributed over the three foot segments. The dynamical equations-of-motion were generated using SD/FAST (PTC, Needham, MA).

The model was driven by 25 Hill-type musculotendon actuators combined into 13 functional groups based on anatomical classification (Fig. 1). Five previously identified activation modules (for details see Neptune et al., 2009) describing time varying activation patterns relative to the gait cycle, were used as the excitation control inputs (Fig. 2). Four of the modules were derived using a non-negative matrix factorization (NNMF) of experimental EMG data (Clark et al., 2009; Neptune et al., 2009) to identify synergistic muscle groups. All muscles, except RF, were assigned to a single module based on the dominant weighting determined by the NNMF. RF, which had approximately equal weighting from two separate modules (Mod 1 and Mod 3), received a net excitation that was the sum of the inputs from both modules. Muscles for which no EMG data were available (GMAX, BFsh and IL) were also assigned to modules based on a post-hoc biomechanical analysis (Neptune et al., 2009). As a result, muscles included in each module were defined as: Mod 1 (VAS, RF, GMAX and GMED), Mod 2 (SOL and GAS), Mod 3 (TA and RF), Mod 4 (HAM and BFsh) and Mod 5 (IL). Due to a lack of EMG data for IL, no module pattern was available. Thus, the IL excitation pattern was modeled using four continuous blocks, or nodes, and characterized by an onset, duration, and a magnitude for each node. For each condition, all muscles within each module received the same excitation pattern and timing as a function of the gait cycle. However, the magnitude within a module was allowed to vary between muscles. Between conditions, timing for each module was also allowed to vary slightly ($\pm 10\%$ of the gait cycle). Block pattern excitations were also used for the remaining small muscles controlling the foot (PR, FLXDG and EXTDG). Activation-deactivation dynamics were modeled with a first-order differential equation (Raasch et al., 1997) with activation and deactivation constants of 12 and 48 ms, respectively.

2.3. Mechanical demand manipulations

The nominal musculoskeletal model was altered to emulate the experimental conditions. For the added weight conditions, the mass and moment of inertia of the trunk segment were increased by 25% of the nominal control model. For the weight support conditions, a constant upward vertical force was applied to the trunk center-of-mass equal to 25% of the control model weight. Finally, for the increased mass only condition, mass and moment of inertia of the trunk segment

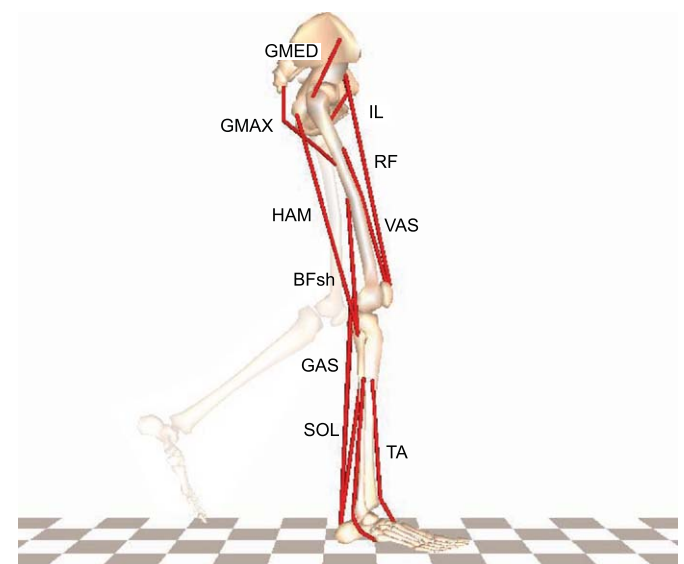


Fig. 1. The musculoskeletal model was made up of rigid segments representing a trunk (head, torso and arms) and two legs, each consisting of a thigh, shank, patella, rear-foot, mid-foot and toes. The model was driven by 25 Hill-type muscle actuators combined into 13 functional groups: IL (iliacus, psoas), GMAX (gluteus maximus, adductor magnus), GMED (anterior and posterior regions of the gluteus medius), VAS (3-component vastus), RF (rectus femoris), HAM (medial hamstrings, biceps femoris long head), BFsh (biceps femoris short head), GAS (medial and lateral gastrocnemius), SOL (soleus, tibialis posterior), TA (tibialis anterior, peroneus tertius), PR (peroneus longus, peroneus brevis), FLXDG (flexor digitorum longus, flexor hallucis longus) and EXTDG (extensor digitorum longus, extensor hallucis longus). For clarity, the small muscles controlling the foot (PR, FLXDG and EXTDG) are not labeled. Muscles for the left leg are not shown.

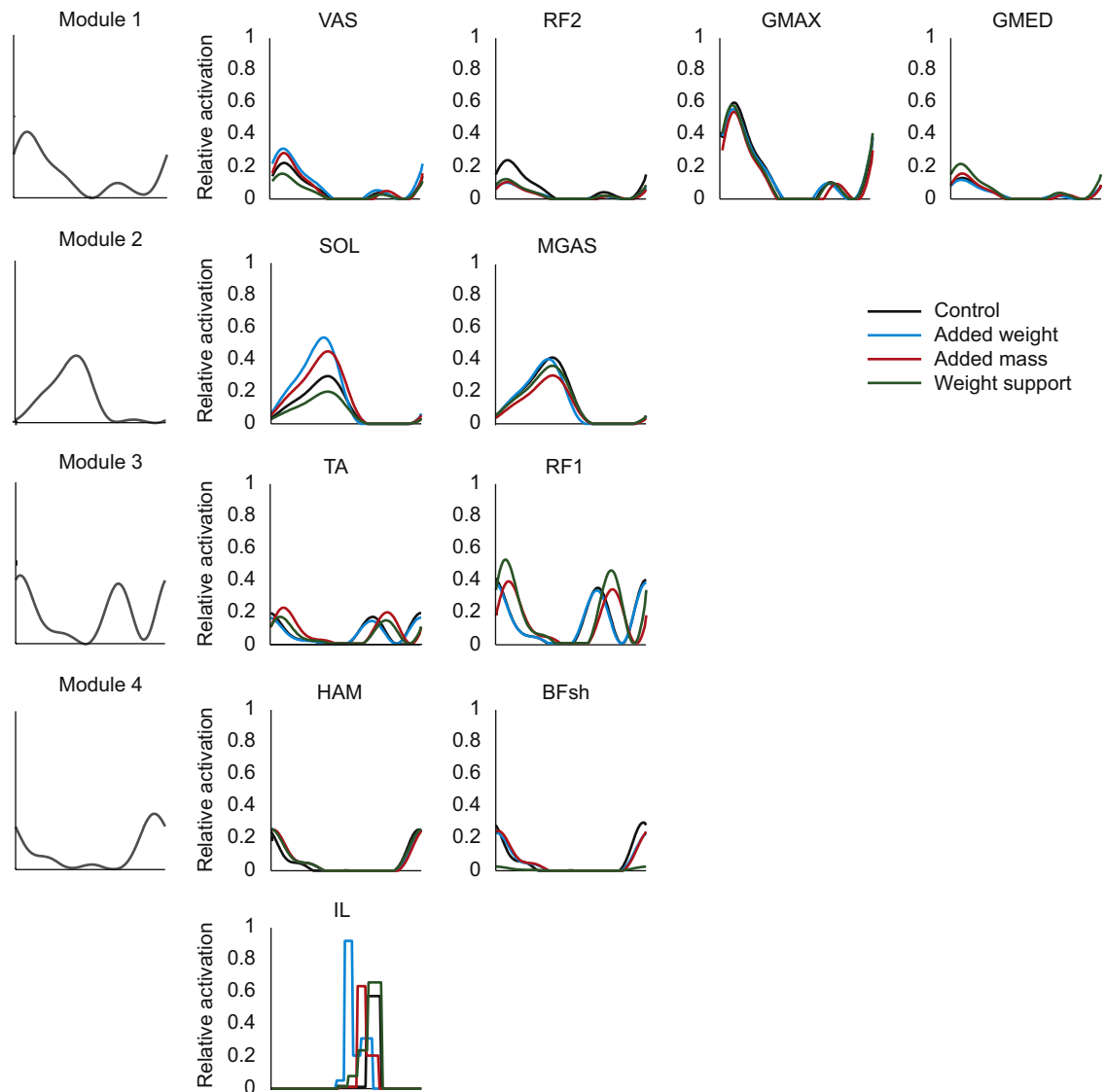


Fig. 2. Experimentally derived module patterns (left column) and the corresponding muscles excited by each module (rows). No experimental data were available for IL, thus a block pattern was used to represent the fifth module (see text for details). The small muscles controlling the foot (PR, FLXDG, and EXTDG) also received individual block patterns and are not shown. For each condition, all muscles within a module received the same excitation timing and pattern, but the magnitude was allowed to vary. Both timing and magnitude were allowed to vary between conditions. The excitation patterns for each condition are plotted for each muscle over a full gait cycle.

were increased as in the added load condition while simultaneously applying an equal constant upward force to the trunk center-of-mass.

2.4. Dynamic optimization

Walking simulations of a complete gait cycle were generated for each condition from left heel-strike to the following left heel-strike. A simulated annealing algorithm (Goffe et al., 1994) was used to fine-tune the muscle excitation patterns and initial joint velocities to minimize the difference between the simulated and experimental data for each condition. The variables tracked included the left and right hip, knee and ankle angles and joint torques, trunk translations (horizontal and vertical) and the horizontal and vertical ground reaction forces. The optimizations were continued until all tracking variables were within two standard deviations of the experimental data.

2.5. Assessing muscle function

To identify the biomechanical functions performed by each module, individual muscle contributions to the GRF and body segment mechanical energetics were determined. Briefly, muscle contributions to the GRFs were quantified by removing one muscle force from the simulation over a 30 ms time interval and computing the change in GRFs for each foot. The change in GRFs was assumed to correspond to the contribution of that muscle to the GRF. Muscle contributions to the body

segment mechanical energetics were determined using a segment power analysis (Fregly and Zajac, 1996), which quantifies each muscle's contribution to the mechanical power of each body segment. Since power is a scalar, power from multiple segments can be summed and analyzed (e.g., power from the leg segments versus the trunk). Each muscle's role in providing body support was assessed by its contribution to the vertical GRF while its role in providing forward propulsion was determined from its contribution to the positive horizontal GRF and positive horizontal trunk power. Contributions to leg swing were determined from the energy delivered to the leg by each muscle during pre and early swing. The contributions by each muscle within a module were then summed to determine each module's contribution to each walking subtask. Contributions by RF to Mod 1 and Mod 3 were scaled based on the relative excitation the muscle received from each module. Detailed descriptions of the GRF decomposition and segment power analyses are provided elsewhere (e.g., Neptune et al., 2004, 2008).

3. Results

3.1. Module patterns and simulation tracking

Using the five previously identified modules as excitation inputs into the musculoskeletal model (Fig. 2), excitation patterns were found that emulated well the experimental data for all

conditions (Fig. 3). Joint angles and normalized ground reaction forces were generally within ± 2 S.D. of the group averaged experimental data with an average error of 1.9° and 0.012 BW, respectively. The simulations also maintained the subject's average walking speed of 1.3 ms^{-1} within $\pm 5\%$ and accounted for minor differences in contact time and duty factor seen among all experimental conditions. The module patterns were allowed to vary between conditions in both timing and magnitude. Differences between conditions were predominantly due to changes in magnitude. However, Mod 3 also exhibited changes in timing during the added mass and weight support conditions (Fig. 2).

3.2. Module contributions to walking subtasks

During all conditions, body support (vertical GRF) was predominantly provided by Mod 1 (VAS, GMAX, GMED and RF) during the first half of stance and Mod 2 (GAS and SOL) during the second half of stance (Fig. 4A). Mod 2 was also the primary

contributor to forward propulsion (positive A-P GRF, Fig. 4B). The muscles controlled by Mod 3 (TA and RF) acted to generate energy to the leg during swing and to decelerate the leg in early and late swing (Fig. 5). Mod 4 (HAM and BFsh) activity added energy to the leg in early stance and acted to decelerate the leg in late swing (Fig. 5). Mod 5 (IL) activity added energy to the leg during pre-swing and swing phases and also transferred energy from the trunk to the leg during swing. The remaining muscles (PR, EXTDG and FLXDG) did not contribute significantly to the mechanical energetics of walking.

The changes in mechanical output associated with each module in response to the experimental perturbations supported our hypotheses. The modules providing body support, Mod 1 and Mod 2, increased their contribution to the vertical GRF during loaded conditions and decreased their contributions during the weight support condition (Fig. 6A). Mod 2, which also provides forward propulsion, increased its contribution to the positive horizontal GRF (Figs. 4B, 6B) and positive horizontal trunk power (Fig. 7) in response to increases in both body weight and mass (added load) and body mass alone. Consistent with our

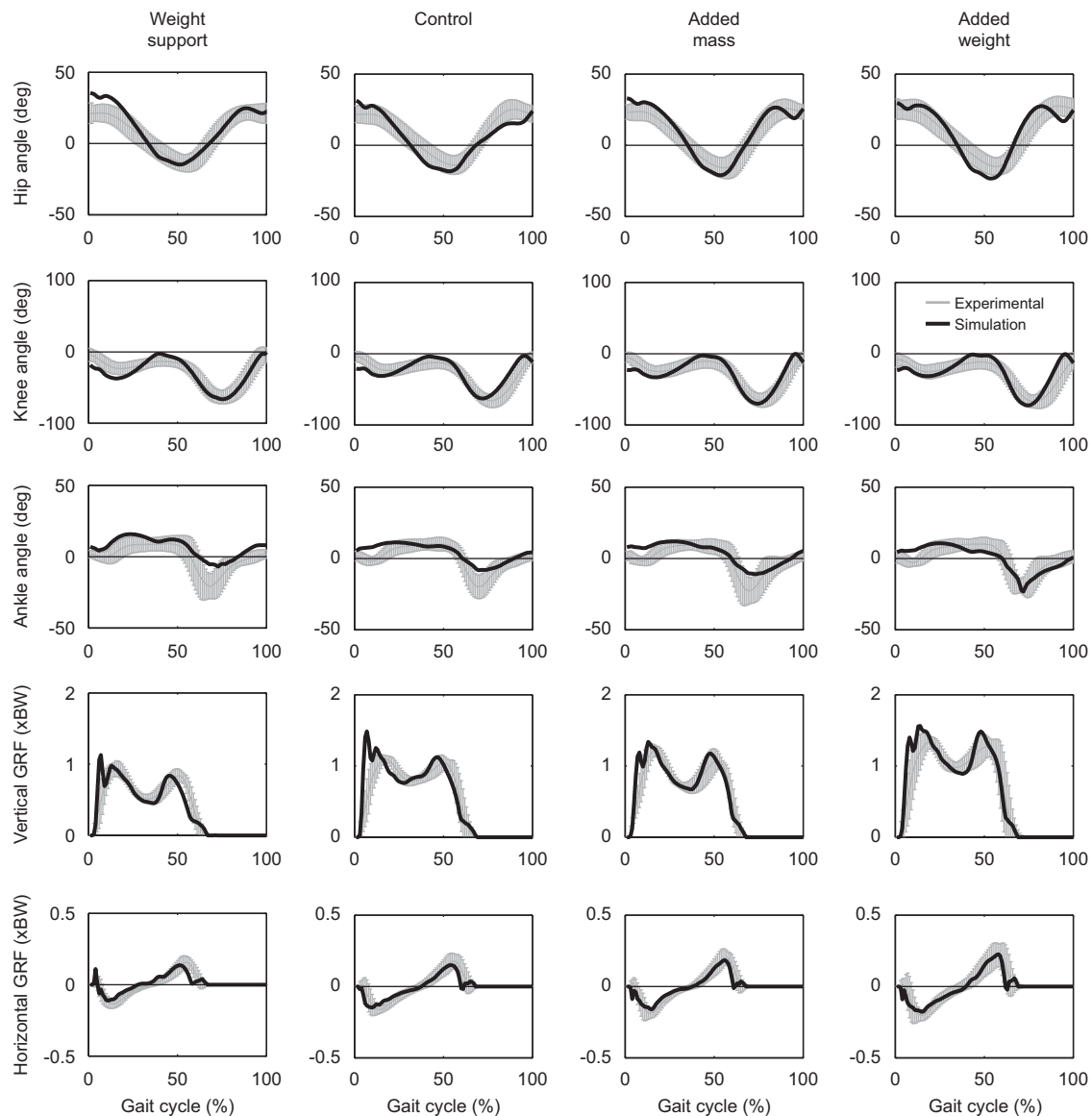


Fig. 3. Tracking results for each simulation condition (columns). The simulated joint angles and ground reaction forces (black) agreed well with the experimental data (grey) during all conditions. The grey regions represent experimental means ± 2 S.D.

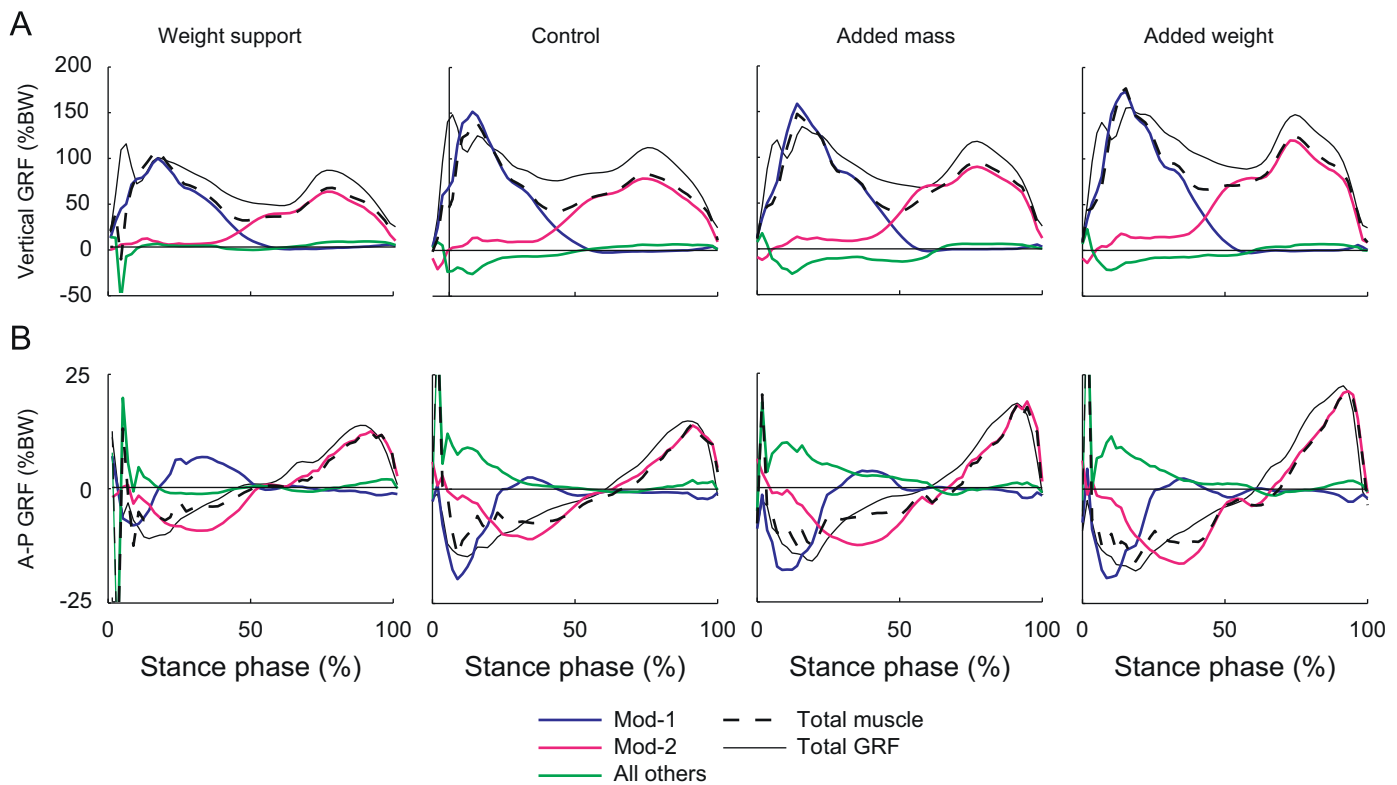


Fig. 4. Module contributions to the simulation (A) vertical and (B) anterior–posterior ground reaction forces. All others includes Mod 3–5 and PR (peroneus longus). Total muscles is the sum of all the muscles.

hypotheses, the modules associated with leg swing (Mods 3–5) were not substantially influenced by the experimental perturbations made to the trunk (Figs. 4, 5).

4. Discussion

A number of studies have provided evidence that the modular control of synergistic muscle groups is associated with specific biomechanical subtasks within a movement. Animal studies have identified reduced sets of patterns that characterize the majority of the variation in muscle excitation during postural and locomotor tasks. In standing cats these patterns have been linked to force production in response to perturbations (Ting and Macpherson, 2005); whereas in kicking frogs, the excitation modules have been associated with controlling the direction of the kick (d'Avella et al., 2003). A recent computer modeling and simulation study of human walking provided strong evidence that individual modules control various walking biomechanical subtasks, such as providing body support or forward propulsion (Neptune et al., 2009).

The experimental protocol in the present study independently altered the demands for specific walking subtasks to further examine the relationships between modules and biomechanical function. The simulation results supported our hypothesis that muscles controlled by modules associated with specific biomechanical tasks would alter their mechanical output in response to changes in demands for that task. Specifically, the modules that provide body support (Mod 1 and Mod 2) increased their contribution to vertical GRF when body weight was increased and decreased their contribution when weight support was applied (Figs. 4, 6). Mod 2, which also provides forward propulsion, increased its contribution to positive A-P GRF (Fig. 6B) and horizontal power acting on the trunk (Fig. 7) during

both added weight and added mass conditions, but remained relatively unchanged during the weight support condition. Because the perturbations were made to the trunk segment and not the leg, we also hypothesized that the modules which predominately function to swing the leg would be largely unaffected by the experimental conditions. This hypothesis was also supported (Fig. 5). These results agree well with our previous study that examined individual muscle responses to manipulations of body weight and body mass in simulations where muscles were excited with individual block patterns (McGowan et al., 2009). In that study we showed that the primary muscles responsible for providing and modulating body support were VAS, GMAX and SOL, whereas the primary muscle providing and modulating forward propulsion was SOL. Interestingly, our previous results showed SOL had the largest contribution in response to both changes in body weight and body mass. This was also the case in the current study, where SOL had greatest changes in excitation magnitude (Fig. 2) and Mod 2 had large changes in response to added weight and added mass (Fig. 6). The results of the current study provide further evidence that these modules can act as basic neural control elements that can be modulated independently to produce well-coordinated walking even when the mechanical demands are significantly altered.

In addition to specific modules responding to changes in the task demands, the relative weighting of muscles within a module were also consistent with experimental data. We previously showed that EMG activity in SOL increased in response to increases in both body weight and body mass and decreased with weight support; whereas GAS activity only increased (decreased) with increased (decreased) body weight (McGowan et al., 2008). We further showed that these relative changes in EMG activity were consistent with each muscle's relative contributions to the walking subtasks of body weight support and forward propulsion (McGowan et al., 2009). It is remarkable

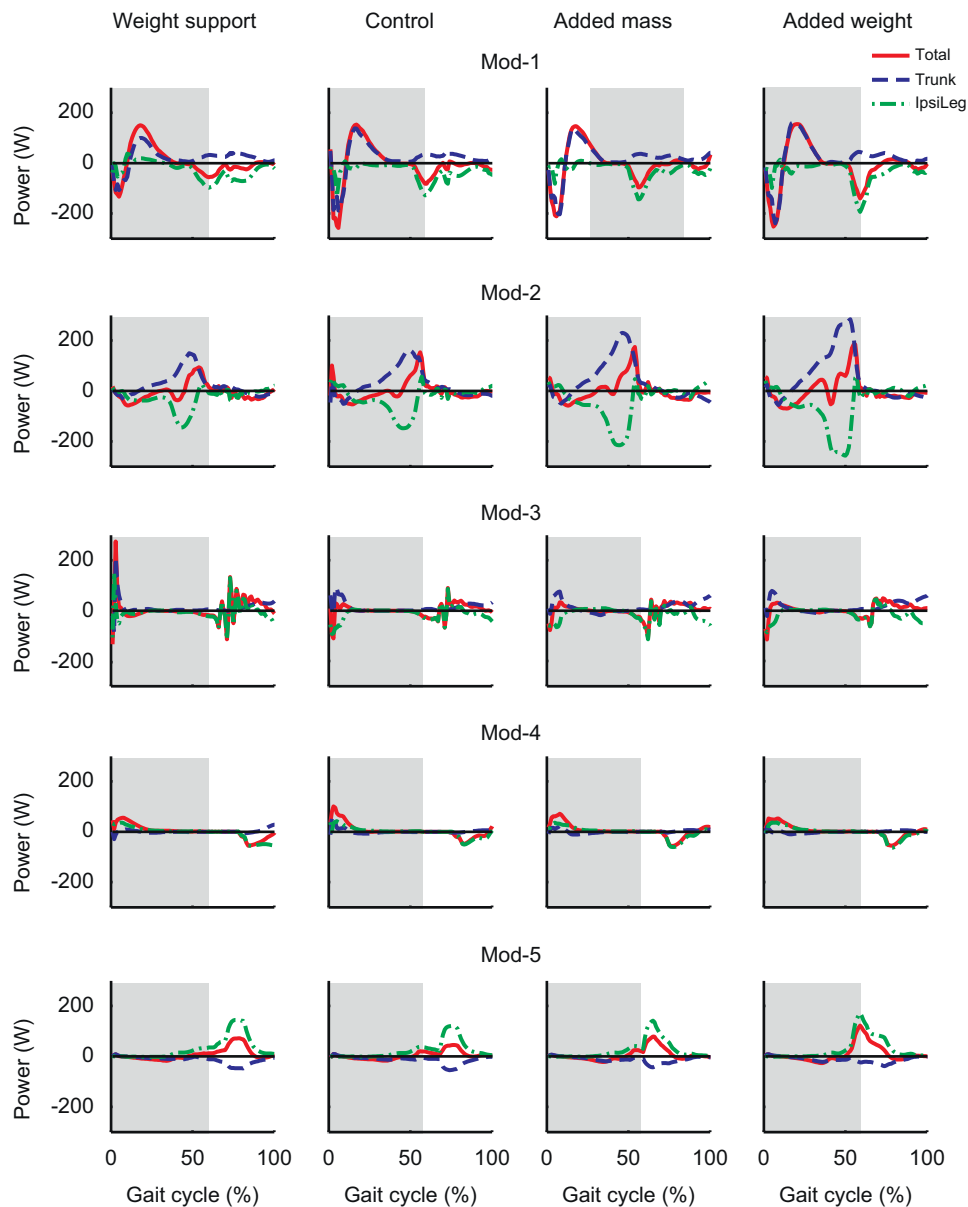


Fig. 5. Mechanical power delivered to the trunk and ipsilateral leg by each module (rows). Total represents the sum of the power delivered to the trunk, ipsilateral and contralateral leg (small, not shown). Positive power and negative power values indicate the module acts to accelerate or decelerate the segment, respectively. The grey shaded region represents stance phase.

that in the present study, tracking the experimental kinematic and kinetic data with no consideration of the EMG data, produced modules with consistent changes in the relative weighting of individual muscles such as SOL and GAS (see Fig. 2). Thus, flexible weightings were required between conditions with substantial changes in mechanical demands in this study, while in our previous study we found that fixed weightings could account for EMG activity over a wide range of speeds (Clark et al., 2009), suggesting less substantial changes in mechanical demand with speed. Note that by allowing the relative level of muscle activations within a module to vary between conditions, we diverged from what has typically been done in other NMF studies (e.g., Bizzi et al., 2008). However, the factorization approach of some others also allow flexibility in weightings (e.g., Ivanenko et al., 2004, 2005) because they do not require consistency in composition or weighting of their modules between conditions in their analyses. This flexibility is also consistent with the concept of synergies proposed by Latash and

colleagues (Latash et al., 2007) who have emphasized that synergies (similar to modules in concept) are task dependent with flexible interrelationships (e.g., muscle weightings) to achieve performance stability and flexibility while dealing with possible perturbations and/or secondary tasks. However, our simulation results suggest that the relative weighting of muscles within a module is not a rigid constraint that is constant over the manipulations of body weight and body mass, instead appearing to be fine-tuned for each condition when necessary.

Although we allowed both the magnitude and timing to change between conditions, differences in module excitation between conditions were predominantly due to changes in magnitude, although Mod 3 exhibited changes in timing during added mass and weight support conditions (Fig. 2). An interesting question is whether the simulation could still emulate well the experimental data if only the magnitude of the module excitations were allowed to vary between conditions without any changes in module timing. We ran a post-hoc simulation of the condition

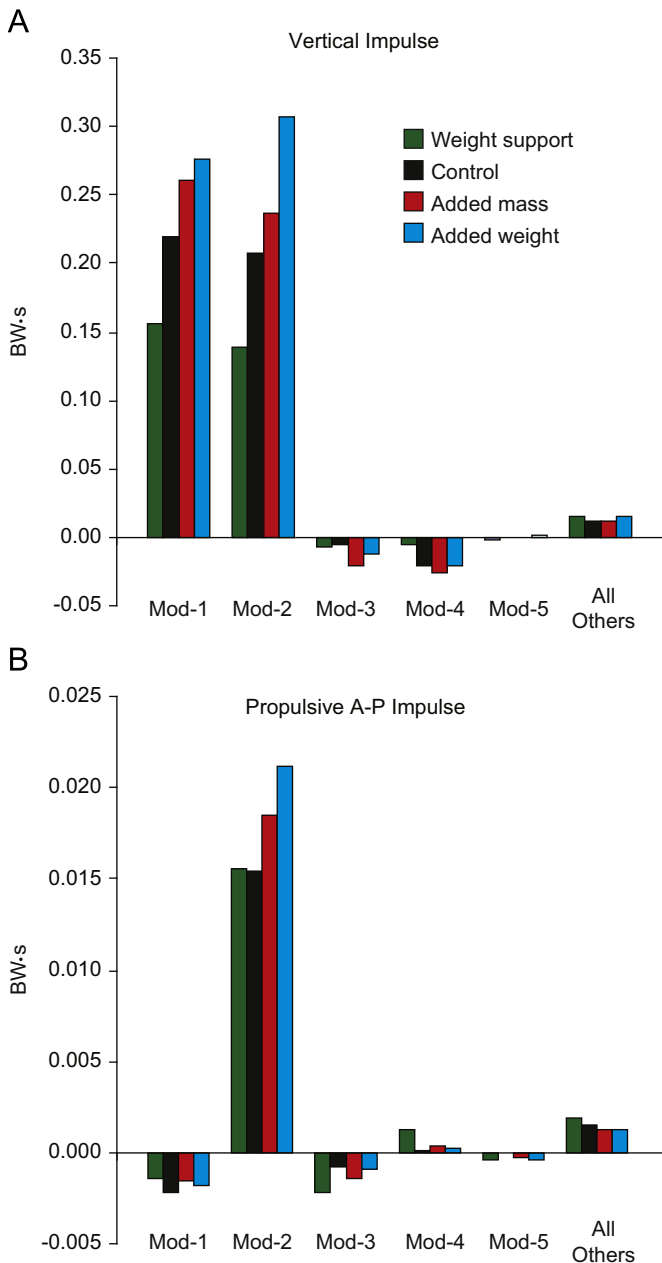


Fig. 6. Module contributions to the vertical and positive anterior–posterior body weight normalized ground reaction force (GRF) impulses during each condition. The vertical impulse was calculated as the time integral of the vertical GRF. The propulsive impulse was calculated as the time integral of the positive anterior–posterior GRF.

that had the greatest timing shift (25% added mass) in which the timing was fully constrained to match that of the control simulation (i.e., the timing was not allowed to change). The results of this simulation produced slightly different GRFs and kinematic patterns, but they matched the experimental data nearly as well as the unconstrained simulation. Average tracking errors for GRFs and kinematics were 0.027 BW and 1.95° for the constrained simulation compared to 0.012 BW and 1.90° for the unconstrained simulation. Thus, despite the small increase in error for the GRFs, the tracking was still well within ± 2 standard deviations of the experimental data. Therefore, it appears that modulation of the module excitation magnitude alone is sufficient to account for the changes in task demands imposed in this study.

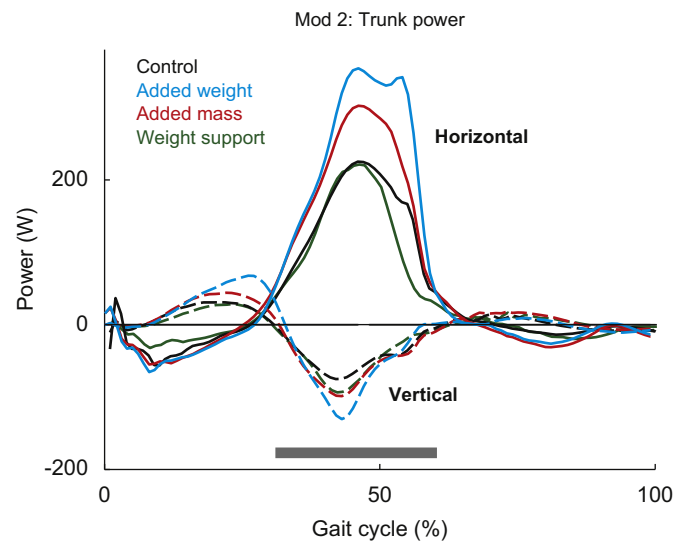


Fig. 7. Contributions from Module 2 to vertical and horizontal trunk power during each condition. The thick grey bar indicates when the trunk is moving down and therefore negative vertical power is contributing to body support by decelerating the downward movement.

In the present study, muscles were assigned a specific module excitation pattern based on previously identified weightings from non-negative matrix factorization (NNMF) of EMG activity during normal walking (Neptune et al., 2009). The results of the NNMF showed that EMG patterns from each muscle consisted of contributions from each module, but the pattern was dominated by a single module (except RF). Therefore, the dominate module was selected to control that muscle during simulations of each condition. It is possible that EMG patterns could change between experimental conditions and thus the weightings for each muscle could also change or additional modules could be identified. However, based on previous analyses of EMG during different experimental conditions (McGowan et al., 2008), it seems unlikely the perturbations used in this study would produce additional modules or that EMG patterns would change enough to alter the assignment of individual muscles to specific modules. Regardless, because we limited the simulations to be controlled by the same set of modules, this study provides a conservative test of whether a reduced set of control modules could reproduce walking when the mechanical demands are altered.

In conclusion, we found that a simple modular control scheme consisting of only five activation patterns was not only able to reproduce well-coordinated walking during normal conditions, but also when the mechanical demands on the system were substantially altered by manipulations of body weight and body mass. Our results support the idea that the nervous system may use a reduced control strategy of activation of a limited number of modules over a broad range of walking tasks and that flexible modulation of recruitment intensity in synergistic muscles within these modules may be sufficient to meet large changes in mechanical demand. Further, the response of individual modules to specific perturbations in this study provided additional compelling evidence for a link between control modules and specific biomechanical subtasks.

Conflict of interest statement

There are no conflicts of interest associated with the manuscript entitled, Modular control of human walking: Adaptations to altered mechanical demands.

Acknowledgements

The authors would like to thank Rodger Kram for help with the experimental data collection. This work was funded by NIH grants RO1 NS55380 and F32 AR054245 and the Rehabilitation Research & Development Service of the VA.

References

- Bizzi, E., Cheung, V.C., d'Avella, A., Saltiel, P., Tresch, M., 2008. Combining modules for movement. *Brain Res. Rev.* 571, 125–133.
- Cappellini, G., Ivanenko, Y.P., Poppele, R.E., Lacquaniti, F., 2006. Motor patterns in human walking and running. *J. Neurophysiol.* 956, 3426–3437.
- Clark, D., Neptune, R.R., Zajac, F.E., Ting, L.H., Kautz, S.A., 2009. Modular organization of muscle activity underlying locomotor control complexity and recovery following stroke. *J. Neurophysiol.* (in press).
- d'Avella, A., Saltiel, P., Bizzi, E., 2003. Combinations of muscle synergies in the construction of a natural motor behavior. *Nat. Neurosci.* 63, 300–308.
- Davis, B.L., Vaughan, C.L., 1993. Phasic behavior of EMG signals during gait: use of multivariate statistics. *J. EMG. Kinesio.* 31, 51–60.
- Fregly, B.J., Zajac, F.E., 1996. A state-space analysis of mechanical energy generation, absorption, and transfer during pedaling. *J. Biomech.* 29 (1), 81–90.
- Goffe, W.L., Ferrier, G.D., Rodgers, J., 1994. Global optimization of statistical functions with simulated annealing. *J. Econometrics* 60, 65–99.
- Grabowski, A., Farley, C.T., Kram, R., 2005. Independent metabolic costs of supporting body weight and accelerating body mass during walking. *J. Appl. Physiol.* 982, 579–583.
- Ivanenko, Y.P., Cappellini, G., Dominici, N., Poppele, R.E., Lacquaniti, F., 2005. Coordination of locomotion with voluntary movements in humans. *J. Neurosci.* 2531, 7238–7253.
- Ivanenko, Y.P., Poppele, R.E., Lacquaniti, F., 2004. Five basic muscle activation patterns account for muscle activity during human locomotion. *J. Physiol.* 556 (Pt 1), 267–282.
- Latash, M.L., Scholz, J.P., Schoner, G., 2007. Toward a new theory of motor synergies. *Motor Control* 113, 276–308.
- McGowan, C.P., Kram, R., Neptune, R.R., 2009. Modulation of leg muscle function in response to altered demand for body support and forward propulsion during walking. *J. Biomech.* 427, 850–856.
- McGowan, C.P., Neptune, R.R., Kram, R., 2008. Independent effects of weight and mass on plantar flexor activity during walking: implications for their contributions to body support and forward propulsion. *J. Appl. Physiol.* 1052, 486–494.
- Neptune, R.R., Clark, D.J., Kautz, S.A., 2009. Modular control of human walking: a simulation study. *J. Biomech.* 429, 1282–1287.
- Neptune, R.R., Sasaki, K., Kautz, S.A., 2008. The effect of walking speed on muscle function and mechanical energetics. *Gait Posture* 281, 135–143.
- Neptune, R.R., Wright, I.C., Van Den Bogert, A.J., 2000. A method for numerical simulation of single limb ground contact events: application to heel-toe running. *Comput. Methods Biomech. Biomed. Eng.* 34, 321–334.
- Neptune, R.R., Zajac, F.E., Kautz, S.A., 2004. Muscle force redistributes segmental power for body progression during walking. *Gait Posture* 192, 194–205.
- Raasch, C.C., Zajac, F.E., Ma, B., Levine, W.S., 1997. Muscle coordination of maximum-speed pedaling. *J. Biomech.* 306, 595–602.
- Ting, L.H., Macpherson, J.M., 2005. A limited set of muscle synergies for force control during a postural task. *J. Neurophysiol.* 931, 609–613.
- Zajac, F.E., Neptune, R.R., Kautz, S.A., 2003. Biomechanics and muscle coordination of human walking: part II: lessons from dynamical simulations and clinical implications. *Gait Posture* 171, 1–17.